17th World Conference on Earthquake Engineering, 17WCEE
Sendai, Japan - September 13th to 18th 2020

Spectral Distribution Estimation Using Super-Dense Observation Records in Tokyo Metropolitan Area

I. Suetomi [1], E. Ishida [2], T. Koyama [3], H. Kimura [4]

[1] *Group Manager, Eight-Japan Engineering Consultants Inc., suetomi-i@ej-hds.co.jp*
[2] *Project Manager, Eight-Japan Engineering Consultants Inc., ishida-e@ej-hds.co.jp*
[3] *Group Manager, Tokyo Gas Co., Ltd., koyama98@tokyo-gas.co.jp*
[4] *Tokyo Gas Co., Ltd., kimura-hiro@tokyo-gas.co.jp*

Abstract

The JMA intensity scale and SI values are often used as judgment criteria of response policy and damage estimation immediately after the earthquake. On the other hand, the predominant period of the surface soil is a very important parameter of the relationship between the earthquake ground motion and damages of the facilities. However, the amplification characteristics of the surface ground are expressed as a function of the Vs30 in the models proposed in the NGA project. Senna and Midorikawa (2009) calculated the average spectrum for the Japan engineering geomorphologic classification based on the spectral amplification using the H/V spectrum of microtremor surveys. There are few models that reflect the spectral amplification using the dominant period.

Tokyo Gas has built a super-dense observation network of about 4,000 in the Tokyo metropolitan area for safe gas supply. In this study, the amplification of the response spectrum is calculated by regression analysis using observed records by the super-dense observation network. Using the 57 earthquakes and 3,776 observation records, regression analysis was performed, and the spectral amplification factor at each site was calculated as the site coefficient.

We propose a function of the spectral amplification factor with two parameters, the predominant period T_1 and the peak amplification factor G_p. Averaged values are calculated for each geological classification. In order to apply this proposed model to the 50m-mesh geology classification data, we constructed 50m-mesh spatial distribution data of T_1 and G_p. In order to confirm this applicability, spectral distribution on the ground surface was estimated with the proposed model, using the observed spectra of the 2005 earthquake in Central- Chiba Prefecture. As a result of comparison with the observed spectrum at the K-NET site, a good result was obtained.

Keywords: Site Amplification, Response Spectra, High Density Observation Records, Tokyo Metropolitan Area, Geological Classification

1. Introduction

Since the ending of the 20th century when large earthquakes have often occurred, the Japan Meteorological Agency (hereinafter referred to as JMA) and NIED started to announce immediately the real-time seismic intensity map in order to support quick decision on the response policy after disaster. SI values are used for the gas supply shutoff criterion in blocks where damages of gas pipelines are severe. Since the seismic response of a structure is strongly affected by its natural period, the period information of the ground motion is important. Therefore, it is desirable to use the response spectrum as the seismic motion index, and it is expected that the damage estimation accuracy will be improved accordingly.

Methods of evaluating the amplification factor of site response using seismic observation records can be broadly classified into 1) regression analysis using dummy variables in order to develop the attenuation relations [1,2], and 2) a method using nearby station pairs[3]. There are many studies on the attenuation relation in the former. In the case of wide area estimation, a spectral amplification model associated with the ground information is required for the amplification evaluation other than the observation point. Although many models have been proposed in the NGA (Next Generation Attenuation relation) project in the U.S.A [e.g., 4, 5, 6], the model forms including the effect of nonlinearity are similar, and the average S-wave velocity up to a depth of 30 m (Vs30) is used as the dominant parameter. Vs30 teaches us whether observation points are on the soft ground or on the hard ground, however, the predominant period of the ground is important in order to evaluate the behavior of the infra-structures. In fact, the amplification factor whose Vs30 is small by the model with Vs30 as a parameter is larger than the factor whose Vs30 is large in the overall periods.

The latter method is mainly used for the purpose of associating the amplified spectrum with Vs30. Yamaguchi and Midorikawa [7] have proposed a method to calculate from Vs30, and Yamaguchi and Midorikawa [8] have proposed a method to consider the effect of nonlinearity. Senna and Midorikawa [9] have proposed the average spectrum corresponding the Japan Engineering Geomorphologic Classification based on the spectral amplification using the H/V spectra of microtremors by the Senna, Midorikawa and Wakamatsu [10].

As noted by Ikeda et al. [11], the basic characteristics, “elongation of predominant period”, that the predominant period during the strong ground motion becomes longer than that of weak motion because of the non-linear behavior of the surface soils should be considered in the amplification models. In this study, therefore, we construct a model that uses the predominant period as a parameter that will be able to be combined with the nonlinear model proposed by Ikeda et al.

Tokyo Gas has operated the super-dense real time monitoring earthquake system "SUPREME" since July 2001. Observed SI values were quickly collected in 5 minutes and damages were estimated during the 2011 Tohoku-Pacific Ocean earthquake. Many observed waveform records have been accumulated. Norito and Inomata [12] estimated the amplification factor of SI value at each observation site and the average factor for geological classification. Suetomi et al. [13] estimated the spectral amplification factor for each strong motion observation site in Yokohama city using the observation point on the rock as a reference point.

In this study, using the observation data at about 4,000 sites more than 30,000 records further accumulated after Norito et al. [14], a new amplification model of acceleration spectra (h=5%), Sa, in the metropolitan area is proposed. The predominant period is used as a dominant parameter in the proposed model, because the borehole data are rich and the number exceeds 60,000. On the other hand, records with strong nonlinearity are scarcely obtained in the metropolitan area, therefore, only linear models are targeted in this paper, and the effects of nonlinearity will be considered in the future.

2. Attenuation relation in the Tokyo metropolitan area

Figure 1 shows the procedure of modelling of site amplification factors in this paper. First, an attenuation relation is estimated by a regression analysis with K-NET data in the Tokyo metropolitan area. Next, spectral ratios of response spectra observed at SUPREME sites to the response spectra at bedrock calculated by the attenuation relation, and the average spectral amplification factor are estimated for observation sites. Then, site amplification model is proposed and parameters are estimated for geological classification by Tokyo Gas.

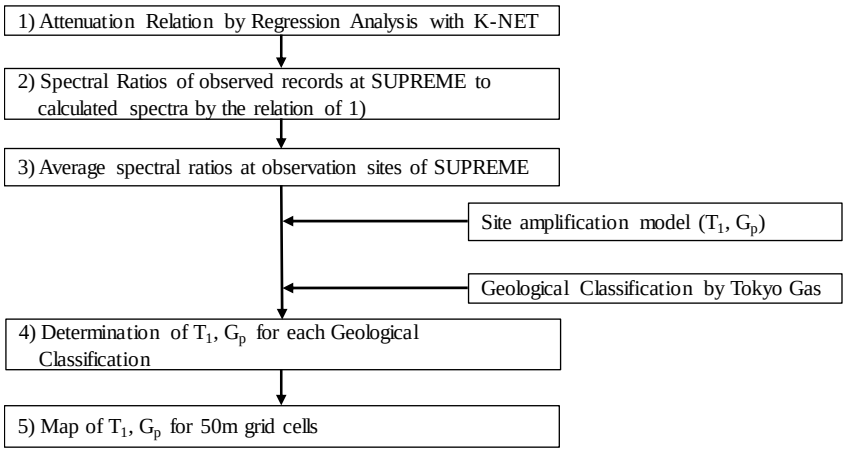

Fig. 1 – Procedure of modelling of site response in this paper

2.1 Earthquakes

Figure 2 shows the epicenter distribution of 57 earthquakes (M>4) that occurred near the Tokyo metropolitan area. It does not include the main shock and the largest aftershock (30 minutes after the main shock) of the 2011 Tohoku-Pacific Ocean Earthquake, which are recorded at many observation points. The reason is that the ground behavior may be nonlinear and the magnitude of the earthquake is much larger than that of other earthquakes.

Table 1 shows the frequency of earthquake magnitude. Most are medium-scale earthquakes around M5.0. Table 2 shows the frequency of the hypocentral depth. There are many earthquakes with a depth of around 60km. The hypocentral information is based on the JMA's "Earthquake and Volcano Monthly Report (Disaster Prevention)".

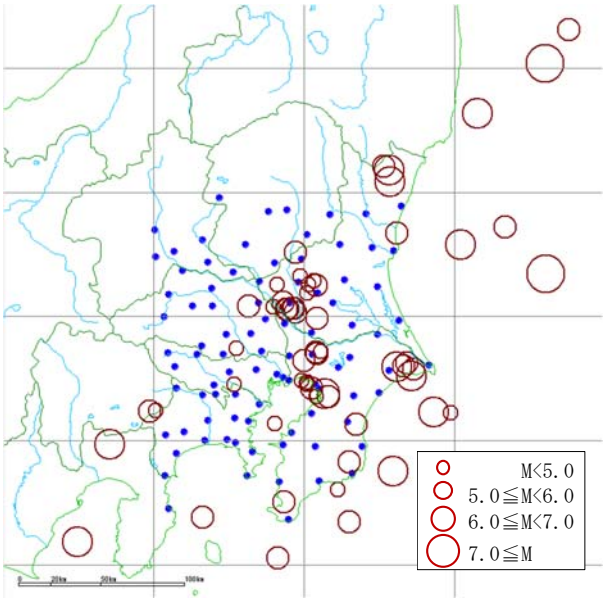

Fig. 2 – Map of Epicenters

Table 1 – Magnitude distribution

Magnitude :M	Number of earthquakes
4≦M＜5	17
5≦M＜6	29
6≦M＜7	10
7≦M	1

Table 2 – Hypocentral depth distribution

Hypocentral depth :D	Number of earthquakes
D＜20	6
20≦D＜40	9
40≦D＜60	26
60≦D＜80	14
80≦D	2

2.2 Regression model

An attenuation relation is constructed by regression analysis of the observation data of 91 points, which added the Yokohama city strong motion observation point "ab03" as a reference point to the K-NET observation point in the metropolitan area. Then, our dataset consists of 4,485 recordings from 53 earthquakes. Since the scale of earthquakes are medium, the following general attenuation equation is used for the regression analysis

$$log_{10}S(T) = a(T) \cdot M + b(T) \cdot X - log_{10}X + c(T) \cdot D + d(T) + \sum_{i=1}^{N} A_i(T) \cdot S_i \quad (1)$$

where $S(T)$: Acceleration response spectra (h=5%)

T : Period (s)

M: JMA Magnitude

X : Hypocentral distance (km)

D : Depth of (km)

S_i : Dummy variable that equals 1 if i=k and zero otherwise

$a(T)$, $b(T)$, $c(T)$, $d(T)$, $A_i(T)$; Regression coefficients

2.3 Results of regression analysis

Figure 3 shows the coefficient of determination R^2. It is large when the period is 1 second or longer, and is small in the short period. Figure 4 shows the coefficient a (T) of the magnitude (M) and the coefficient b (T) of the distance (X). It is considered that a (T) gradually increases with the period, and that the effect of the distance decreases as the period becomes longer.

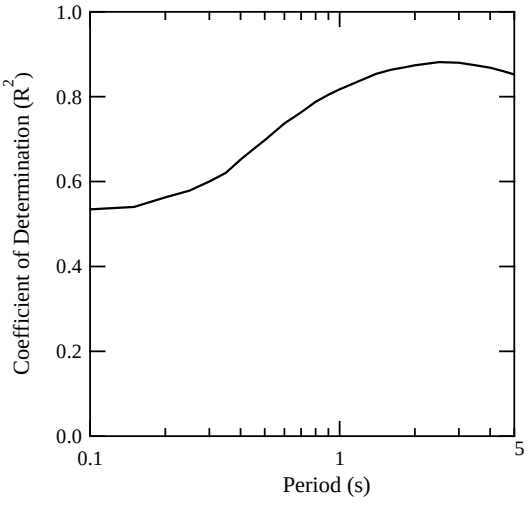

Fig. 3 - Coefficient of determination

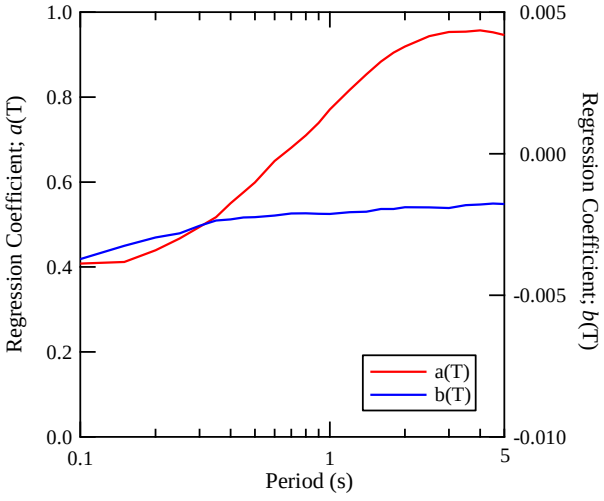

Fig. 4 - Regression coefficient $a(T)$ and $b(T)$

2.4 Spectral Ratios at the Site of SUPREME

For each observation point of Tokyo Gas, the spectral ratios to engineering bedrock are calculated for observed earthquake ground motion records using the above-mentioned attenuation relation for all observation sites of SUPREME. Next, the average spectra are calculated for the sites that satisfy the condition that 3 or more

waveform records out of 53 earthquakes have been obtained. Examples of spectral amplification factors of acceleration response spectra (h=5%) are shown in Figure 5. The geology of each observation point is as follows. The site of No.20227 is in “Flood plain in valley”, No. 21041 is in “Delta and coastal l”, No.21126 is in “Reclaimed land and filled land”, No.20419 is in “Flood plain”, No.20398 is in “Musashino terrace”, No.389 is in “Valley bottom lowland”. Since amplification factors are calculated as the ratios to the attenuation relation, it can be seen that the predominant periods are stable, although the variation of spectral ratios is large.

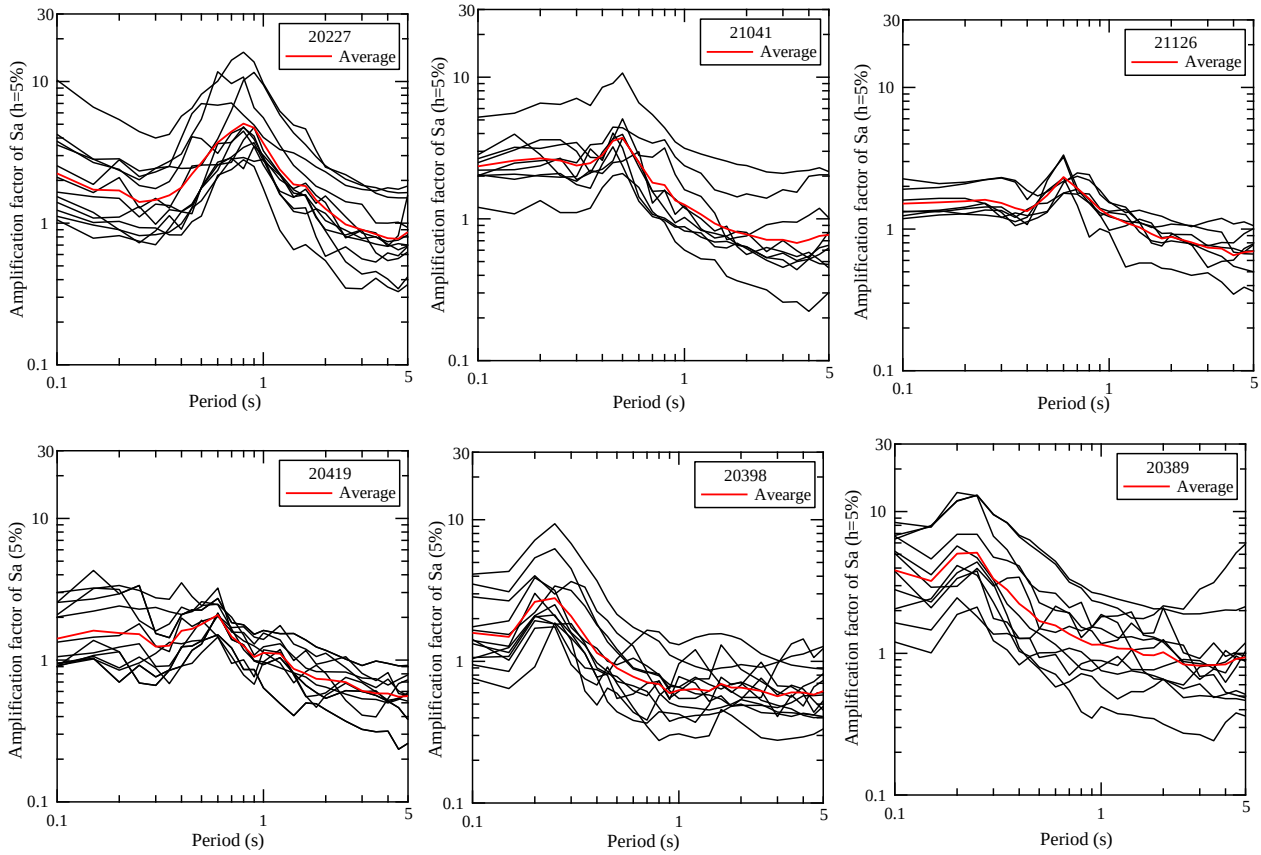

Fig. 5 – Examples of spectral amplification factors of Sa (h=5%)

3. Spectral Amplification Model and Geological Classification

In this study, we focus on the observation points that have three or more waveform data among the target earthquakes and 3,776 points including the reference point.

The geological classification map by Tokyo Gas is based on the Geographical Survey Institute's land condition map and added some classifications in consideration of the topography in the metropolitan area. Table 3 shows the classification and Fig. 5 shows the distribution map.

Figure 6 shows the average spectral amplification factors for each geological classification. It can be seen that the peaks become smoother when averaged, but there are observation points that show distinct peaks individually. Geological classification is roughly divided into hills (orange in Table 3) and lowlands (blue in Table 3). The predominant periods of the amplification spectra of hills are less than 0.3 seconds, and the predominant periods of those of lowland are around 0.7 seconds. That of valley bottom lowland has an intermediate value between the two because the surface layer is thin.

Table 3 – Geological classification and average predominant period of site response

Geological classification	Predominant period: T_1	Peak value: G_p
Sloping land	0.188	7.41
Hills	0.188	7.31
Shimosueyoshi terrace	0.172	7.28
Musashino terrace	0.207	6.08
Tachikawa terrace	0.118	6.65
Natural levee	0.729	6.15
Sand dune	0.754	3.98
Valley bottom lowland	0.261	5.47
Delta and coastal lowland	0.774	6.32
Back marsh	0.767	5.36
Abandoned river channels	0.664	6.32
Flood plain	0.745	7.02
Flood plain in valley	0.390	5.02
Dry riverbed	0.722	5.66
Artificially modified land	0.187	4.89
Reclaimed land and filled land	0.858	5.12
Embankment at alluvial lowland	0.238	4.64

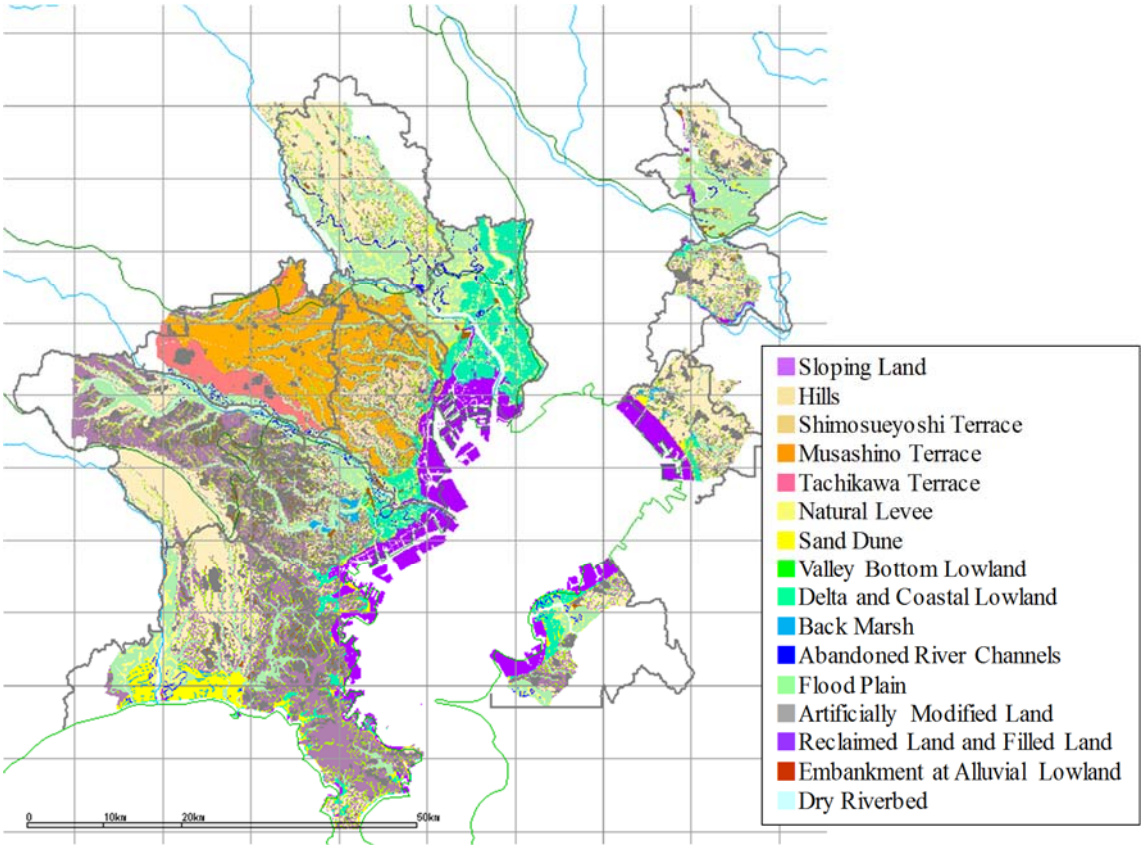

Fig. 6 – Geological Classification in the Tokyo metropolitan area by Tokyo Gas

In this paper, the following equation is used to determine the spectral amplification with reference to the site amplification factor *Gs* by the revised Building Standard Law of 2000 [15]. Two parameters, predominant period T_1 and peak value G_p, are estimated using amplification spectra with observed records.

$$\begin{aligned} T \leqq 0.8T_2 \quad & G_S=1.0 \\ 0.8T_2<T \leqq 0.8T_1 \quad & G_S=1.0+\frac{G_P-1}{0.8(T_1-T_2)}(T-0.8T_2) \\ 0.8T_1<T \leqq 1.2T_1 \quad & G_S=G_P \\ 1.2T_1<T \quad & G_S=G_P+\frac{G_P-1}{\frac{1}{1.2T_1}-0.1}\left(\frac{1}{T}-\frac{1}{1.2T_1}\right) \end{aligned} \tag{2}$$

where $T_2=T_1/3$.

T_1 and G_p are average values of each geological classification are shown in the right column of Table 3, and the amplification spectra using Eq. (2) with these parameters are shown in Figure 6.

4. Parameters of 50m mesh in the Tokyo metropolitan area

The proposed model is represented by two parameters, a predominant period (T_1) and a peak value (G_p). Then, the combining method by Suetomi et al. [16] which calculates Vs30 by weighting Vs30 based on topographic classification and Vs30 based on boring data is adopted in order to construct 50m-mesh amplification data by calculating two parameters by spatial interpolation in this paper. The amplification spectra of 50m-meshes are calculated by Eq. (2) with two parameters.

Fig. 7 shows the predominant period, and Fig. 8 shows the distribution of peak values. The difference of the predominant period between the lowlands and the hills is clear in Fig. (a). The predominant periods at the hillside are around 0.2 seconds, and those at the lowlands are more than 0.6 seconds. The predominant periods around the Arakawa estuary and the Tama estuary are longer than those at other lowlands in Fig. (b) combined with the seismic observation points. It is considered that the effect of layer thickness, which cannot be considered only by topographic classification, is expressed. The peak values are not much different at around 5 times in Fig. (a), but those have a wide range from 3 to 10 times in Fig. (b). The peak values at lowlands are about 4 times and those of the hillside are larger in Fig. 8.

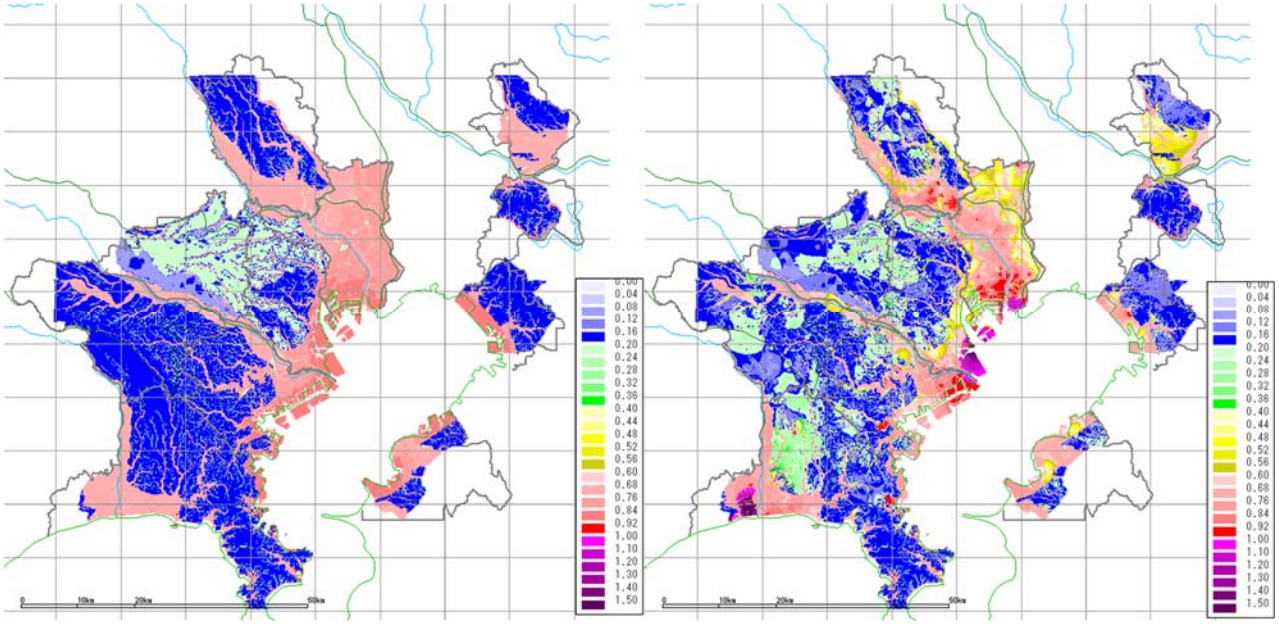

(a)Geological classification model (b)Proposed combined model

Fig. 7 – Map of predominant period; T_1

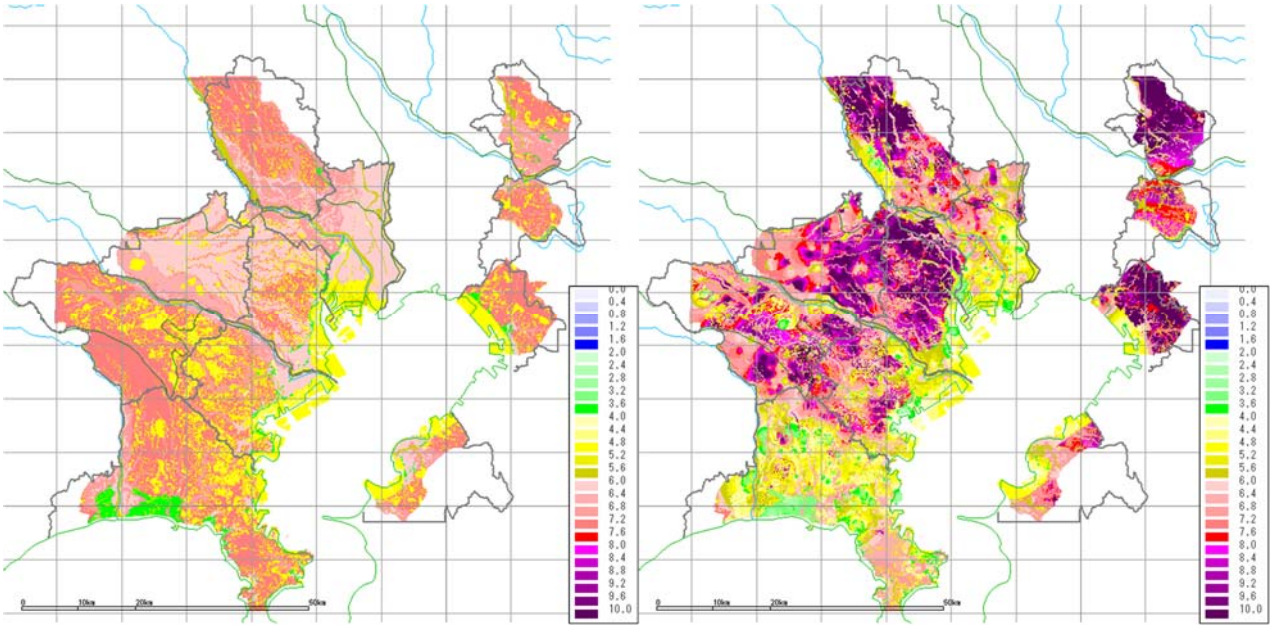

(a)Geological classification model (b)Proposed combined model

Fig. 8 – Map of peak value; G_p

5. Case Study for the 2005 Central-Chiba earthquake

The accuracy is verified by comparing the interpolated estimation results with the observation records of other organizations in the actual observed earthquake. The observation records during the M6.0 earthquake which occurred in Central-Chiba Prefecture on July 23, 2005, are used for the case study, since the model proposed in this paper is a linear model. Using the observed records by the SUPREME system and the amplification factors of the proposed model, response spectra on the engineering base are calculated. Next, the distribution map of response spectra on the engineering base is calculated by an interpolation using the IDW method and the acceleration response spectra on the ground surface are calculated with the amplification factors by T_1 and G_p of 50m-meshes.

Figure 9 shows the distribution of the maximum acceleration response at the periods of 0.5 and 1.0 seconds. The areas where the acceleration responses are large at 0.5 seconds are widely seen near the border between Tokyo and Saitama Prefecture and near Sodegaura City in Chiba Prefecture. The shear wave velocities of the surface ground are small and the surface layers are thick in the areas.

Figure 10 shows comparison examples of the observed specta and the estimated spectra at the K-NET observation sites which are not used for the interpolation analysis. The solid black line is the acceleration response spectrum (h=5%) of the earthquake record actually observed at the target observation point, and the solid red line is the result of interpolation estimation using the proposed amplification model. The geology of each observation point is as follows. TKY016 and CHB009 are in “Reclaimed land and filled land”, TKY021 and KNG001 are in ”Delta and coastal lowland”, TKY006 is in “Musashino terrace”, KNG003 is in “Artificially modified land”.

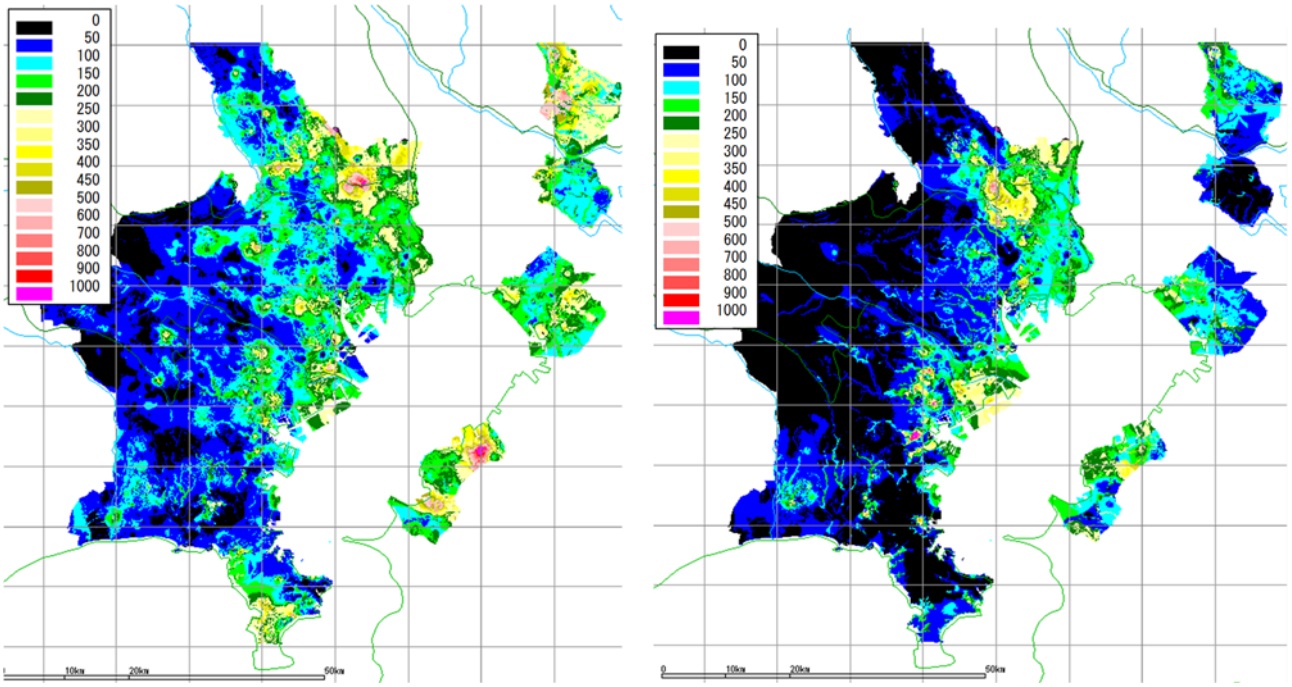

(a)T=0.5s (b)T=1.0s

Fig. 9 – Map of Sa during the 2005 Central Chibaearthquake (M_J=6.0)

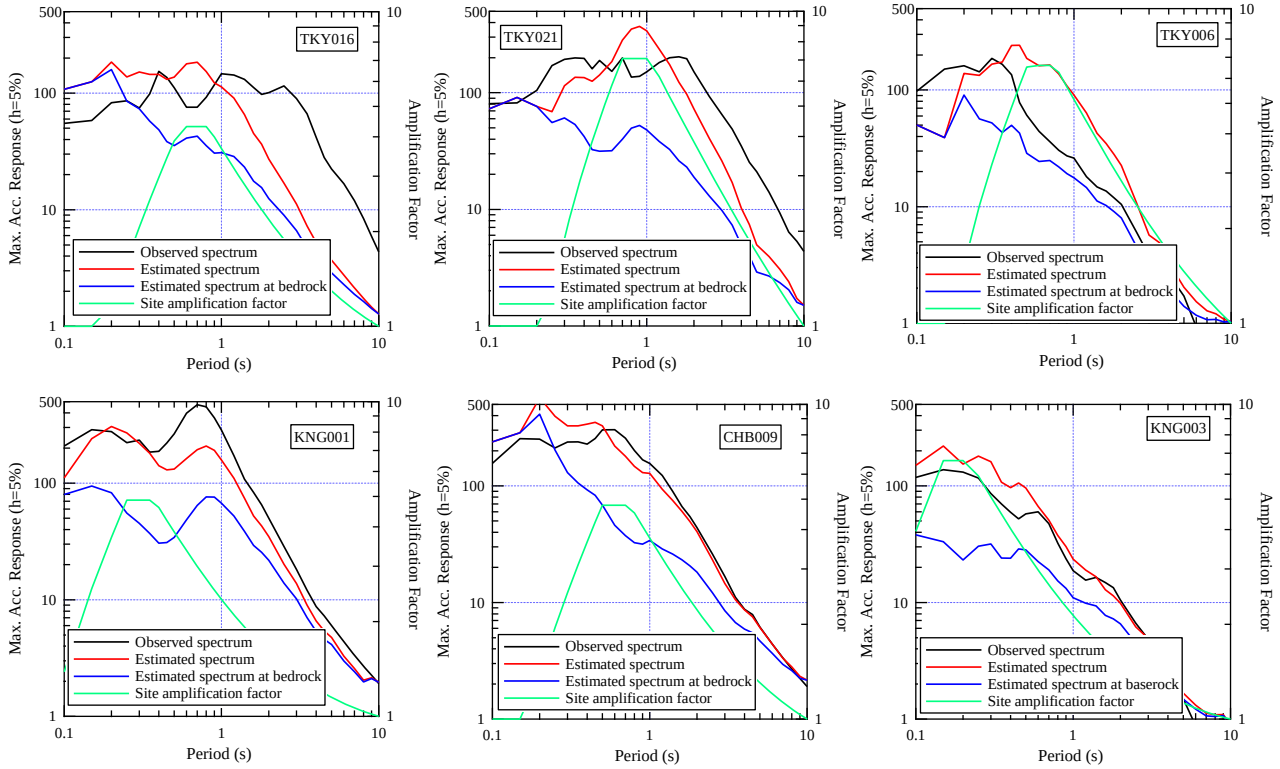

Fig. 10 – Comparison between observed spectra and estimated spectra at K-NET sites

6. Concluding Remarks

In this paper, we proposed a function of the spectral amplification factor with two parameters, the predominant period T_1 and the peak amplification factor G_p. In order to confirm this applicability, spectral distribution on the ground surface was estimated with the proposed model, using the observed spectra of the 2005 earthquake in Central-Chiba Prefecture. The principal conclusions are as follows:

1) A regression analysis of the acceleration response spectra (h= 5%) recorded at the Tokyo Gas high-density seismic observation was performed with the dummy variables, and the amplification spectra were calculated as the ratios to acceleration responses at the engineering bedrock by the estimated attenuation relation.

2) The average spectral ratio of each Tokyo Gas geological classification was calculated using the results of the regression analysis. We proposed an amplification model which has 2 parameters, the predominant period T_1 and the peak amplification factor G_p and set the parameters for each geological classification.

3) Using the geological classification of the 50m-mesh by Tokyo Gas and the average amplification spectra at the observation sites, spatial interpolation was performed for the predominant period and the peak amplification factor with the weight of the distance, respectively, and the data set of the amplification spectra of the 50m-mesh was constructed.

4) The distribution of Sa was estimated for the 2005 Central-Chiba earthquake, and the applicability of the proposed model was confirmed by comparing K-NET observations with the estimated spectra.

In the future, we will work on nonlinear problems.

7. Acknowledgements

Strong ground motion data used in this study were provided by NIED and Yokohama city. We would like to thank all the contributors of these data.

8. References

[1] Kamiyama M, Yanagisawa E (1986): A statistical model for estimating response spectra with emphasis on local soil conditions, *Soils and Foundations*, **26**(2), 16-32.

[2] Kanno T, Narita A, Morikawa N, Fujiwara H, Fukushima Y (2006): A new attenuation relation for strong ground motion in Japan based on recorded data, *Bull. Seism. Soc. Am.*, **96**, 879-897.

[3] Fujimoto K, Midorikawa S (2006): Relationship between average shear-wave velocity and site amplification inferred from strong motion records at nearby station pairs, *Journal of JAEE*, **6**(1), 11-22 (in Japanese).

[4] Abrahamson NA, Silva WJ (1997): Empirical response spectral attenuation relations for shallow crustal earthquakes, *Seismological Research Letters*, **68**(1), 94-127.

[5] Boore DM, Stewart JP, Seyhan E, Atkinson GM (2014): NGA-West2 equations for predicting PGA, PGV, and 5% damped PSA for shallow crustal earthquakes, *Earthquake Spectra*, **30**(3), 1057-1085.

[6] Chiou BSJ, Youngs RR (2014): Update of the Chiou and Youngs NGA model for the average horizontal component of peak ground motion and response spectra, *Earthquake Spectra*, **30**(3), 1117-1153.

[7] Yamaguchi M, Midorikawa S (2011): Improvement of Method for Estimation of Site Amplification Factor Based on Average Shear-wave Velocity of Ground, *Journal of JAEE*, **11**(3), 85-101 (in Japanese).

[8] Yamaguchi M, Midorikawa S (2014): Empirical models for nonlinear site amplification evaluated from observed strong motion records, *Journal of JAEE*, **14**(1), 56-70 (in Japanese).

[9] Senna S, Midorikawa S, Wakamatsu K (2008): Estimation of spectral amplification of ground using H/V spectral ratio of microtremors and geomorphological land classification, *Journal of JAEE*, **8**(4), 1-15 (in Japanese).

[10] Senna S, Midorikawa S (2009): Estimation of spectral amplification of ground motion based on geomorphological land classification, *Journal of JAEE*, **9**(4), 11-25 (in Japanese).

[11] Norito Y, Inomata W (2012): Result of SUPREME (Super-dense real time monitoring earthquake system for city gas supply) in "Tohoku region Pacific coast earthquake", 15th WCEE, Lisbon, No.1496.

[12] Suetomi I, Fukushima Y, Ishida E, Inomata W, Norito Y, Yamazaki F, Suzuki T (2012): Precision of spatial interpolation estimation of response spectra using the records observed by Yokohama dense array, *Journal of Japan Society of Civil Engineers, Ser. A1 (Structural Engineering & Earthquake Engineering (SE/EE))*, **68**(4), 126-137 (in Japanese).

[13] Norito Y, Inomata W, Suetomi I, Ishida E, Yamazaki F, Suzuki T (2014): Site amplification factor estimated with super-dense array observation in capital region, *Journal of Japan Society of Civil Engineers, Ser. A1 (Structural Engineering & Earthquake Engineering (SE/EE))*, **70**(4), 520-526 (in Japanese).

[14] Ikeda T, Katoh K, Ishida H (2018): Nonlinear site amplification modeling of response spectra using strong ground motion records, *Journal of JAEE*, **18**(2), 130-146 (in Japanese).

[15] The Building Center of Japan (2000): The building standard law of Japan.

[16] Suetomi I, Ishida E, Fukushima Y, Isoyama R, Sawada S (2007): Mixing method of geomorphologic classification and borehole data for estimation of average shear-wave velocity and distribution of peak ground motion during the 2004 Niigata-Chuetsu earthquake, *Journal of JAEE*, **7**(3), 1-12 (in Japanese).